

Measuring individual tree crown diameter with lidar and assessing its influence on estimating forest volume and biomass

Sorin C. Popescu, Randolph H. Wynne, and Ross F. Nelson

Abstract. The main objective of this study was to develop reliable processing and analysis techniques to facilitate the use of small-footprint lidar data for estimating tree crown diameter by measuring individual trees identifiable on the three-dimensional lidar surface. In addition, the study explored the importance of the lidar-derived crown diameter for estimating tree volume and biomass. The lidar dataset was acquired over deciduous, coniferous, and mixed stands of varying age classes and settings typical of the southeastern United States. For identifying individual trees, lidar processing techniques used data fusion with multispectral optical data and local filtering with both square and circular windows of variable size. The crown diameter was calculated as the average of two values measured along two perpendicular directions from the location of each tree top by fitting a fourth-degree polynomial on both profiles. The lidar-derived tree measurements were used with regression models and cross-validation to estimate plot level field-measured crown diameter. Linear regression was also used to compare plot level tree volume and biomass estimation with and without lidar-derived crown diameter measures from individual trees. Results for estimating crown diameter were similar for both pines and deciduous trees, with R^2 values of 0.62–0.63 for the dominant trees (root mean square error (RMSE) 1.36 to 1.41 m). Lidar-measured crown diameter improved R^2 values for volume and biomass estimation by up to 0.25 for both pines and deciduous plots (RMSE improved by up to 8 m³/ha for volume and 7 Mg/ha for biomass). For the pine plots, average crown diameter alone explained 78% of the variance associated with biomass (RMSE 31.28 Mg/ha) and 83% of the variance for volume (RMSE 47.90 m³/ha).

Résumé. L'objectif principal de cette étude était de développer des techniques fiables de traitement et d'analyse pour faciliter l'utilisation des données lidar à petite empreinte dans le contexte de l'estimation du diamètre de la couronne des arbres en mesurant les arbres individuels identifiables sur la surface lidar tri-dimensionnelle. De plus, l'étude a permis d'explorer l'importance du diamètre de la couronne dérivé du lidar dans l'estimation du volume et de la biomasse des arbres. L'ensemble de données lidar a été acquis au-dessus de peuplements de feuillus, de conifères et de forêt mixte de classes d'âge et de milieux variables typiques du sud-est des États-Unis. Pour l'identification des arbres individuels, les techniques de traitement lidar ont fait appel à la fusion des données impliquant des données optiques multispectrales et le filtrage local avec des fenêtres carrées et circulaires de dimension variable. Le diamètre de la couronne a été calculé comme étant la moyenne de deux valeurs mesurées le long de deux directions perpendiculaires à partir de la localisation de chaque sommet d'arbre en ajustant un polynôme du quatrième degré sur les deux profils. Les mesures d'arbres dérivées du lidar ont été utilisées avec des modèles de régression et la validation croisée pour estimer le diamètre de la couronne mesurée au sol au niveau de la parcelle. La régression linéaire a également été utilisée pour comparer les estimations du volume des arbres et de la biomasse au niveau de la parcelle avec et sans les mesures du diamètre de la couronne dérivées du lidar des arbres individuels. Les résultats de l'estimation du diamètre de la couronne étaient similaires pour les pins et les feuillus, avec des valeurs de R^2 de 0,62–0,63 pour les espèces dominantes d'arbres (RMSE de 1,36 à 1,41 m). Le diamètre de la couronne mesuré par lidar a amélioré les valeurs de R^2 dans l'estimation du volume et de la biomasse de plus de 0,25 pour les parcelles de pins et de feuillus (la valeur de RMSE s'est améliorée de jusqu'à 8 m³/ha pour le volume et de 7 Mg/ha pour la biomasse). Pour les parcelles de pins, le diamètre moyen de la couronne permettait à lui seul d'expliquer 78 % de la variance associée à la biomasse (RMSE de 31,28 Mg/ha) et 83 % de la variance dans le cas du volume (RMSE de 47,90 m³/ha).

[Traduit par la Rédaction]

Received 17 July 2002. Accepted 23 May 2003.

S.C. Popescu¹ and R.H. Wynne. Department of Forestry, Virginia Tech, 319 Cheatham Hall (0324), Blacksburg, VA 24061, U.S.A.

R.F. Nelson. Biospheric Sciences Branch, NASA – Goddard Space Flight Center, Code 923, Building 33, Room G405, Greenbelt, MD 20771, U.S.A.

¹Corresponding author. Present address: Spatial Sciences Laboratory, Department of Forest Science, Texas A&M University, 1500 Research Parkway, Suite B223, College Station, TX 77845, U.S.A. (e-mail: s-popescu@tamu.edu).

Introduction

In recent years, the use of airborne lidar technology to measure forest biophysical characteristics has been rapidly increasing. In addition to providing a characterization of ground topography, lidar data give new knowledge about the canopy surface and vegetation parameters, such as height, tree density, and crown dimensions, which are critical for environmental modeling activities. Airborne lidar data combine both surface elevations and accurate planimetric coordinates, and processing algorithms can identify single trees or groups of trees to extract various measurements on their three-dimensional representation.

The foundations of lidar forest measurements lie with the photogrammetric techniques developed to assess tree height, volume, and biomass. Aerial stand volume tables are based on estimates of two or three photographic characteristics of the dominant-codominant crown canopy: average stand height, average crown diameter, and percentage of crown closure (Avery and Burkhart, 1994). Such tables are derived by multiple regression analysis with independent variables measured on photographs by skilled interpreters. Forest measurements on photographs covering large areas can become a tedious endeavor and rely to some degree on the interpreter's ability. Since it is generally not feasible to measure and count every tree in the area of interest, a sampling process analogous to field procedures is often used. The height and density of forest stands can also be estimated on large-scale digital airborne imagery because there exists a close link between the three-dimensional organization of the canopy and image texture (St-Onge and Cavayas, 1995). The image spatial structure is only a two-dimensional representation of forest structure. In contrast, lidar pushes traditional remote sensing image processing for forest applications into the three-dimensional domain by being able to provide a unique metric, the vertical dimension of the canopy. Lidar characteristics, such as high sampling intensity, extensive areal coverage, ability to penetrate beneath the top layer of the canopy, precise geolocation, and accurate ranging measurements, make airborne laser systems useful for directly assessing vegetation characteristics.

Previous studies that focused on estimating forest stand characteristics with scanning lasers used lidar data with either relatively large laser footprints, 5–25 m, (Harding et al., 1994; Lefsky et al., 1997; Weishampel et al., 1997; Blair et al., 1999; Lefsky et al., 1999; Means et al., 1999) or small footprints, but with only one laser return (Næsset, 1997a; 1997b; Magnussen and Boudewyn, 1998; Magnussen et al., 1999). Early studies used lidar data to estimate forest vegetation characteristics, such as percent canopy cover, biomass (Nelson et al., 1984; 1988a; 1988b; Nelson, 1997), and gross-merchantable timber volume (Maclean and Krabill, 1986). Small-footprint lidars are available commercially and research results on their potential for forestry applications are very promising. As more systems operate with high performance, research into forestry applications of lidar has become very intense and resulted in a

series of studies that demonstrate that lidar technology is well suited for providing estimates of forest biophysical parameters (Næsset and Bjercknes, 2001; Holmgren et al., 2002; Næsset and Økland, 2002; Popescu et al., 2002; Popescu, 2002; McCombs et al., 2003; Popescu and Wynne, 2003). Despite the intense research efforts, practical applications of small-footprint lidar have not progressed too far, mainly because of the current cost of lidar data. In addition, lidar studies have concentrated on measuring what lidar is best suited for, measuring tree heights and deriving other biophysical parameters using height metrics. With the increased detail currently afforded by new lidar data and an anticipated decline of lidar data cost in the near future, lidar is expected to be used extensively in forest measurements.

One of the tree dimensions that can be directly measured with lidar is crown diameter, but currently there is a lack of lidar literature on this subject. In a simulation study, Popescu et al. (2000) derived the average crown width using canopy closure and stand density as predictors. Average crown area can be estimated by dividing the canopy area, i.e., number of laser canopy pixels multiplied by the area of one pixel of the interpolated canopy height model, by the number of stems. The average crown diameter for the whole stand is then indirectly computed assuming a circular crown with the area equal to average horizontal crown area. Other direct approaches to the detection of individual tree crowns using high spatial resolution optical imagery are valley following (Gougeon, 1999), edge finding (Pinz, 1999), morphology (Barbezat and Jacot, 1999), semivariograms, and slope breaks (Wulder et al., 2000).

This study explored the feasibility of using multiple return, small-footprint lidar data for estimating tree crown diameter. The primary purpose of this research was to develop a lidar processing procedure for measuring crown diameter that takes advantage of the ability of small-footprint scanning lasers to portray the canopy structure down to the individual tree level. The specific objectives of this study were (i) to develop reliable processing and analysis techniques to facilitate the use of small-footprint lidar data for predicting plot level average crown diameter by directly measuring individual trees identifiable on the three-dimensional lidar surface; (ii) to explore the influence of different processing methods for locating individual trees on estimating crown diameter; and (iii) to investigate the usefulness of lidar-derived crown diameter in addition to other lidar-measured parameters, such as tree height and number of trees, to estimate forest biomass and stand volume.

Materials and methods

Study site

The study area is located in the southeastern United States (37°25'N, 78°41'W), in the Piedmont physiographic province of Virginia (**Figure 1**). It includes a portion of the Appomattox–Buckingham State Forest that is characterized by deciduous, coniferous, and mixed stands of varying age classes. A mean

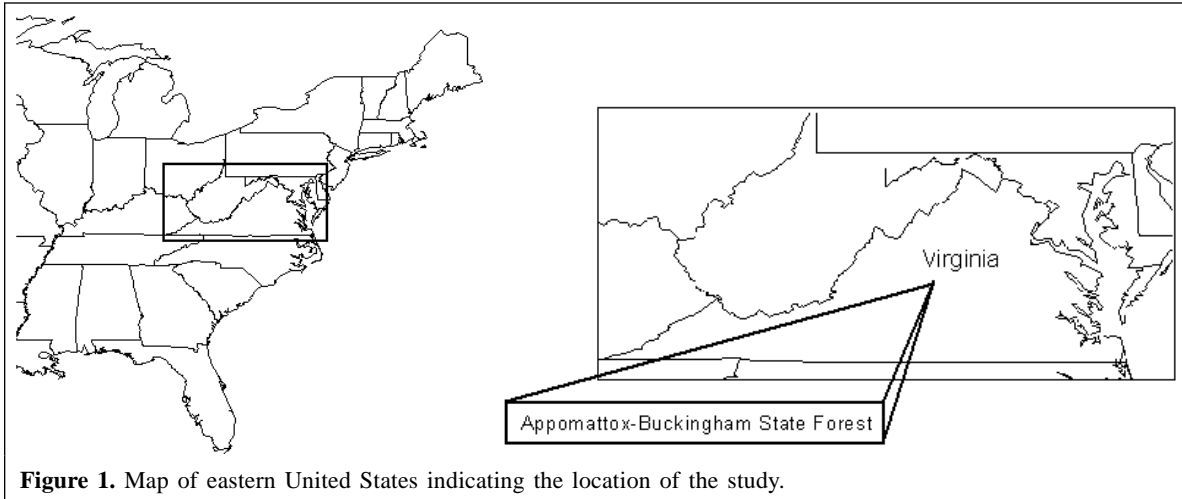


Figure 1. Map of eastern United States indicating the location of the study.

elevation of 185 m, with a minimum of 159 m and a maximum of 238 m, and rather gentle slopes characterize the topography of the study area.

Ground inventory data

The ground truth data were collected from November 1999 to April 2000. Six forest vegetation types were covered by the field sampling — pine hardwoods, upland hardwoods, bottomland hardwoods, and stands of loblolly pine, Virginia pine, and shortleaf pine. Forest type is a plot-level classification defined by the relative stocking of tree species or species groups (Powell et al., 1993). The stand age varied, being approximately 15 years for the majority of the pine stands, 35 to 55 years for the pine-hardwood mixed stands, 85 to 90 years for the bottomland hardwoods, and 100 to 140 years for the upland-hardwood stands. Three stands of loblolly pine were exceptionally old at 60–65 years. A more detailed description of the tree species inventoried on the ground can be found in Popescu (2002) and Popescu et al. (2002).

The plot design followed the U.S. National Forest Inventory and Analysis (FIA) field data layout (Figure 2). An FIA plot consists of a cluster of four subplots approximately 0.017 ha (0.04 acres) each, with a radius of 7.32 m (24.0 ft) (U.S. Department of Agriculture – Forest Service, 2001). One plot is distributed over an area of approximately 0.4 ha (1 acre), thus it represents a sample of the conditions within this area. The center plot is subplot 1. Subplots 2, 3, and 4 are located 36.58 m (120.0 ft) at azimuths 0°, 120°, and 240° from the center of subplot 1. Subplots are used to collect data on trees with a diameter at breast height (dbh) (diameter measured at 1.37 m (4.5 ft) above the ground) of 12.7 cm (5.0 in) or greater. A total of 16 plots were measured in the study area, each with 4 subplots. FIA plot centers (subplot 1 centers) were located systematically on a 200 m × 200 m grid (656 ft × 656 ft), with rows oriented east–west and columns oriented north–south (Figure 3). The origin of the grid relative to the map was randomly selected. Plots were selected to ensure representation of the forest cover types in the study area while concomitantly

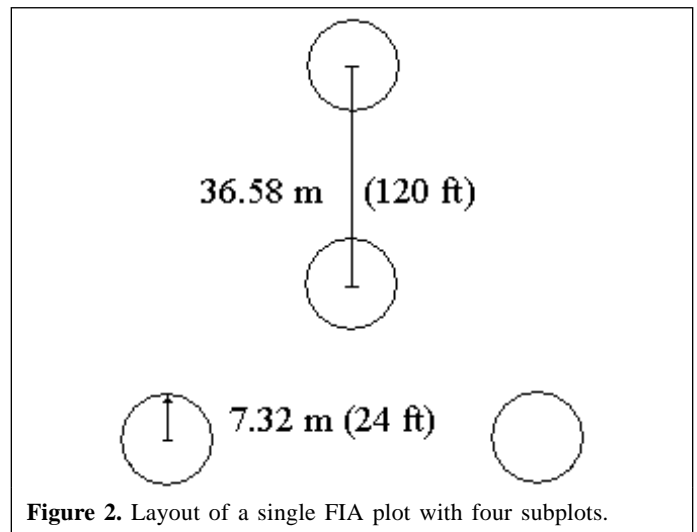


Figure 2. Layout of a single FIA plot with four subplots.

maintaining approximate equivalence between the number of coniferous and deciduous plots (Table 1).

To simplify the analysis relative to tree species, subplots have been categorized as either “hardwoods” or “pines”. For the pine-hardwoods mixed stands, the species group of the subplot was named after the predominant tree species. Predominance was established by basal area (Eyre, 1980) and the subplot category was assigned to the species comprising more than half of the stocking. The ground-truth dataset contained 33 hardwood subplots and 31 pine subplots.

The centers of subplots 1, for most of the plots, were laid out in the field using a navigational global positioning system (GPS) unit — PLGR (Rockwell Collins, Cedar Rapids, Iowa). Centers of subplots 2, 3, and 4 of the same plot were located by bearing and distance from subplot 1. All FIA subplot locations were determined using 60-s static measurements with a 12-channel GPS receiver, HP-GPS-L4 with a PC5-L data collector (Corvallis Microtechnology, Inc., Corvallis, Ore.). The reported mapping accuracy for the HP-GPS-L4 unit, obtained under open sky for 60 s of static measurements, is 30 cm (Corvallis Microtechnology, Inc., 2001). Under forest canopy, GPS systems tend to yield from 1.5 to 3 times less accurate

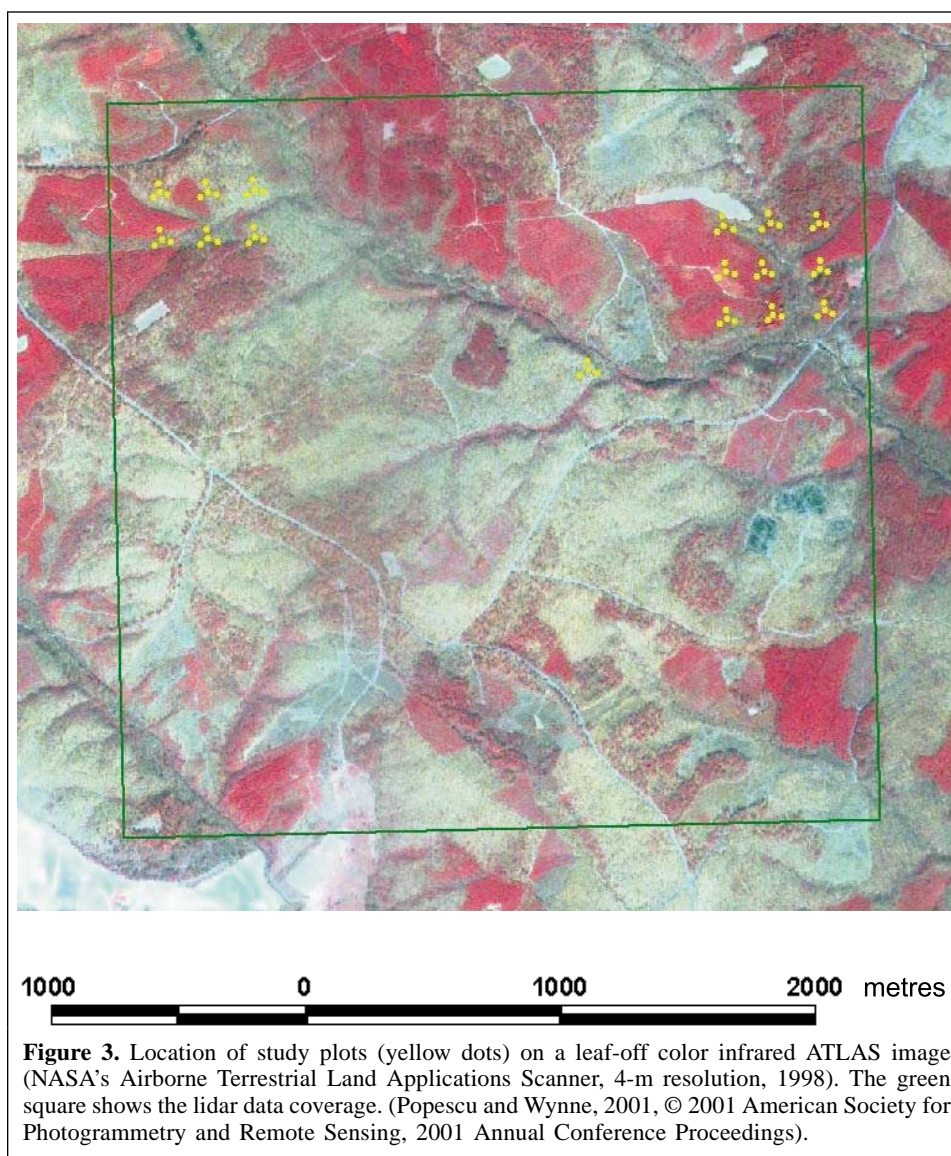


Figure 3. Location of study plots (yellow dots) on a leaf-off color infrared ATLAS image (NASA's Airborne Terrestrial Land Applications Scanner, 4-m resolution, 1998). The green square shows the lidar data coverage. (Popescu and Wynne, 2001, © 2001 American Society for Photogrammetry and Remote Sensing, 2001 Annual Conference Proceedings).

Table 1. Number of subplots differentiated by forest cover type.

Forest cover type	No. of subplots
Pine-hardwood	14
Upland hardwood	17
Bottomland hardwood	7
Total hardwood and mixed pine-hardwood	38
Loblolly pine	16
Virginia pine	6
Shortleaf pine	4
Total pines	26
Total number of subplots	64

solutions (C. Greenwald, Corvallis Microtechnology, Inc., Technical Support, 2001, personal communication). Therefore, we estimated sub-meter accuracy for locating the plot centers.

A more in-depth discussion of the ground measurements and the instruments used to acquire them is given in Popescu (2002) and Popescu et al. (2002).

On each subplot, crown width was measured on all trees with a dbh larger than 12.7 cm (5.0 in). Crown width was determined as the average of four perpendicular crown radii measured with a tape from the tree bole towards the subplot center, away from it, to the right, and to the left. Subplot averages were calculated from individual tree measurements and were used to assess the performance of the lidar processing algorithms. Descriptive statistics of subplot values for the pines and deciduous plots are given in **Table 2**.

The standards for FIA data collection (i.e., acceptable errors in quality checks, though check crews were not used in this study) refer to measurements of tree height and mapping, but not to crown width. However, the error of measuring crown diameter on the ground, to the full extent of the individual crowns, is estimated to be at 0.6–0.9 m (2–3 ft).

Table 2. Descriptive statistics of the field inventory data for pines and deciduous subplots.

Statistic	dbh (cm)	Height (m)	Crown width (m)	No. of trees/plot
Pines				
Mean	13.22	10.56	4.04	21.90
Min.	7.57	5.03	1.97	3
Max.	26.67	17.37	10.12	68
SD	4.21	2.98	1.79	13
Deciduous plots				
Mean	17.18	12.99	5.98	11.3
Min.	8.42	8.58	3.79	3
Max.	28.88	18.64	8.85	22
SD	4.30	2.18	1.27	5

Note: SD, standard deviation.

Lidar dataset

The lidar data were acquired on 2 September 1999 over an area of 1012 ha (2500 acres) located in the Appomattox–Buckingham State Forest in Virginia, U.S.A. The lidar system (AeroScan, EarthData, Inc., Frederick, Md.) utilizes advanced technology in airborne positioning and orientation, enabling the collection of high-accuracy digital surface data. For the Appomattox–Buckingham dataset, the scanning angle was 10°, giving a total field of view of 20°. The average ground swath width was 699 m and the entire research area was covered by 21 parallel flight lines. A more detailed description of the lidar dataset and the sensor characteristics is given in Popescu et al. (2002). The laser beam divergence was of 0.33 mrad, producing a footprint of 0.65 m from the flying height of 1980 m. The reported accuracies for the AeroScan lidar system flying at less than 2400 m above ground, over open homogeneous flat terrain, are as follows: an elevation or vertical accuracy of ± 25 cm and a horizontal accuracy of ± 50 cm (EarthData, Inc., 2003).

The mission was designed with up to 70% sidelap to increase the point density on the ground and to correct for the typical zigzag lidar scanning. By pooling all the laser points from adjacent swaths into the same point file, the average interpoint distance decreased to 0.7 m. For this study only the first and the last returns were used. The last return could coincide with the first, if there is only one return per pulse, or could be any other return from the second to the fourth, depending on the number of returns for a particular pulse.

Popescu and Wynne (2003) investigated the laser point density for this lidar dataset on a regular grid of 1 m \times 1 m cells; therefore the statistical measures were reported directly per square metre. The distribution of the number of points per square metre is summarized in **Table 3**.

Optical data

In addition to the lidar data, spatially coincident optical data used for this study included a leaf-off ATLAS image (NASA's

Table 3. Basic statistical measures for the number of lidar points per 1 m².

Statistic	Value
No. of 1 m ² cells analyzed	435 600
Mean	1.35
Mode	1
Median	1
SD	1.89
Range	54
Interquartile range	2

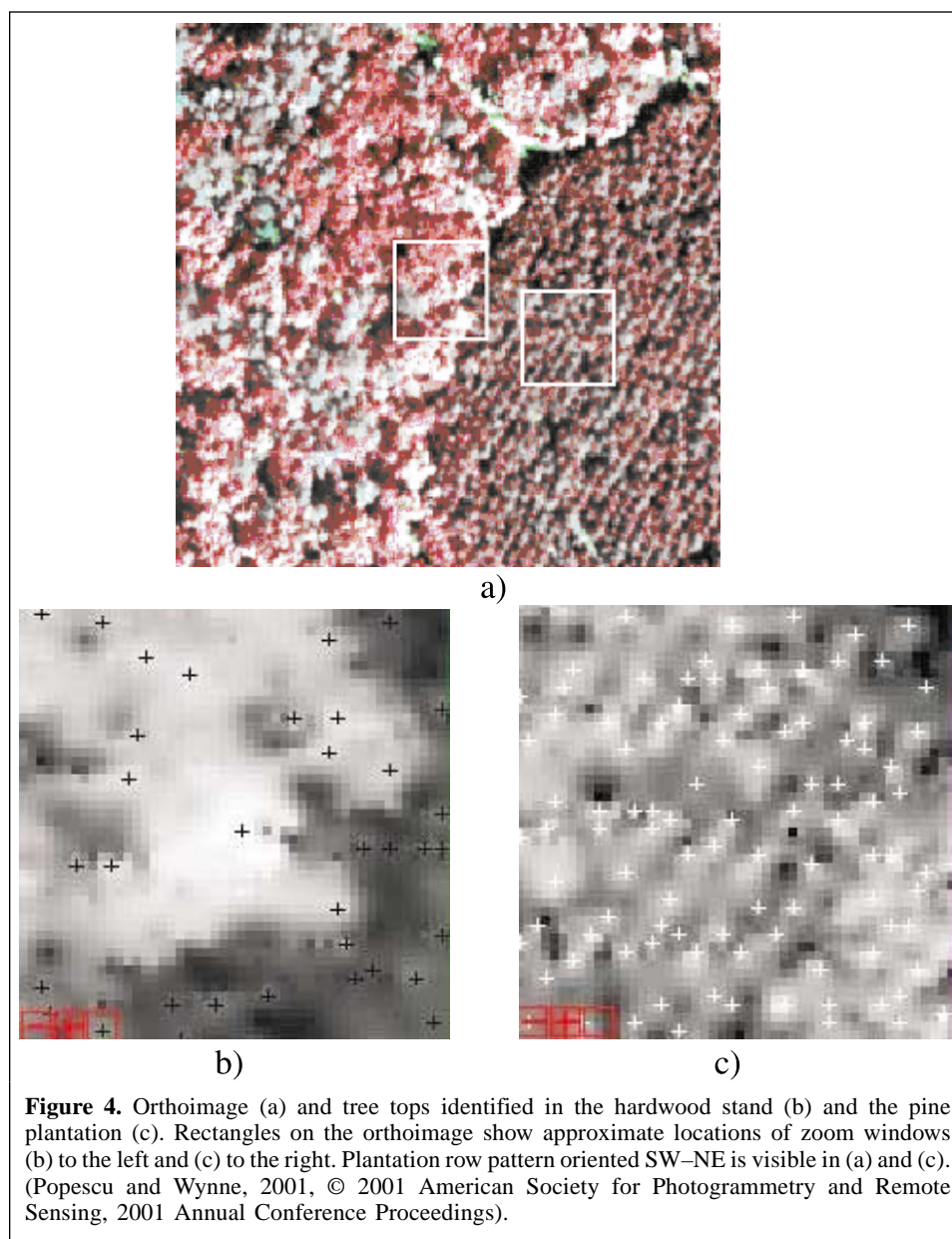
Airborne Terrestrial Land Applications Scanner; 4-m spatial resolution; flown 17 March 1998 at 2100 m AGL), shown in **Figure 3**. The ATLAS image was coregistered to an orthoimage (**Figure 4a**) provided by EarthData, Inc., and derived from 1:13 800 color-infrared photography acquired by NASA in the fall of 1999 (0.5-m spatial resolution).

Canopy height model

The tree canopy height model (CHM) was computed as the difference between tree canopy hits and the corresponding digital elevation model (DEM) values. Tree canopy hits or first-return lidar points were interpolated to a regular grid that corresponds to the digital surface model (DSM). To take advantage of the lidar point density that allows a three-dimensional surface representation of individual trees, the grid size of the DSM of first-return lidar points was 0.5 m. More details about creating the top surface of the forest vegetation canopy are given in Popescu and Wynne (2003).

Locating individual trees

This study only investigated the effect of processing methods for locating the trees on estimating crown diameter. An in-depth description of the lidar processing techniques for locating individual trees that involves focal filtering with variable window size, with both square and circular filter shape, and data fusion with optical imagery is given in Popescu and Wynne (2003). To summarize, the local maximum (LM) technique used to locate trees in this study operates with two shapes of the search window, specifically a square $n \times n$ window and a circular window that is more appropriate to identify tree crowns. The algorithm was implemented in IDL Version 5.5 (Research Systems, Inc., Boulder, Colo.). The LM technique operates on the assumption that high laser values in a spatial neighborhood represent the tip of a tree crown. A similar technique with variable window size and texture analysis was used by Daley et al. (1998) with high-resolution optical images (MEIS-II) to estimate crown position in stands of Douglas fir (*Pseudotsuga menziesii* (Mirb.) Franco). Variable window sizes were also used by Wulder et al. (2000) for the extraction of tree locations and estimation of basal area from high spatial resolution imagery for stands of Douglas fir and western red cedar (*Thuja plicata*). With an image spatial resolution of 1 m, they used window sizes (in metres) of 3 \times 3, 5 \times 5, and 7 \times 7.



The variable window sizes assigned to each pixel were based on the semivariance range or local breaks in slope.

The derivation of the appropriate window size to search for tree tops is based on the assumption that there is a relationship between the height of the trees and their crown size. The higher the trees, the larger the crown size. Thus, tree height and crown size data from the field inventory were used to derive a relationship between tree height and crown size. The relationship between crown width and tree height was investigated separately for the two species categories, pines and deciduous trees, and also for the combined dataset (Popescu and Wynne, 2003). Since lidar data with only height measurements do not offer adequate information to distinguish between tree species, data fusion with the leaf-off ATLAS image was used to differentiate between the two categories of species, deciduous and coniferous. The image was classified

into three classes: open ground, deciduous, and coniferous. The classified image was spatially coregistered to the lidar data and resampled to the smaller grid size of the lidar surface. Therefore, the fused dataset contained information on canopy height and tree species group and allowed a better calibration of the filtering window size based on tree species and height. With this method of locating trees and measuring their height, lidar measurements explained 97% of the variance associated with the mean height of dominant trees for the pine plots and 79% for the deciduous plots.

Based on these relationships and the CHM heights, the window size varied between 3×3 and 31×31 pixels, which corresponds to crown sizes between 1.5 and 15.5 m. The maximum crown diameter measured on the ground belonged to a white oak tree and was 13.8 m. In the case of the circular window for the LM filter, the window diameter varied between

the same limits mentioned above for the size of the regular square windows.

Individual trees were located on the CHM with circular and square window LM filters, with and without data fusion with optical data for each of the filter shapes. Once the location of each identified tree crown is established for each of the filtering methods, the canopy three-dimensional surface of laser heights (CHM) is sampled only at the positions of the tree apex to find out the height of each tree. The variable window size LM technique that identifies tree tops was also used to estimate the number of trees per plot and thus, the stand density.

Crown diameter

The algorithm developed for this study uses the location of individual trees (Figure 4) identified with the LM filter. A 3×3 median filter was used with the CHM to avoid some of the noise in the highly complex surface representing the top of the canopy. The median filter was favored, since it is useful for noise suppression without affecting original values in the CHM. Also, it is an edge preserving filter (Erdas Inc., 1997), better suited for conserving the delineation between adjacent tree crowns.

The crown diameter is the average of two values measured along two perpendicular directions from the location of the tree top. To describe the crown profiles along the two directions on the CHM, the algorithm fits on both profiles a fourth-degree polynomial with least squares by use of the singular value decomposition (SVD) method (Press et al., 1992). The length of each of the two profiles is limited to twice the window size and is centered on the tree top. The fourth-degree polynomial allows the corresponding function to have a concave shape along the crown profile of a single tree, with three extreme values. An extreme value corresponds in most of the cases to either a local maximum or minimum of the fitted function (Gillett, 1984). The values of the independent variable at extreme functional values are known as the critical points. The independent variable in this case is the distance along the vertical profile through the CHM and the dependent variable is the CHM height. The sign of the first derivative indicates whether the graph of the fitted function is rising or falling. The first derivative is equal to zero at extreme values. The sign of the second derivative, negative or positive, indicates respectively whether the graph of the fitted function is concave or convex and whether a critical point is a local maximum or minimum. Points of inflection occur where the concavity of the fitted function changes. The algorithm (Figure 5) finds the critical points of the fitted function and analyzes the extreme values they yield, based on the first and second derivatives. Numerical differentiation with 3-point Lagrangian interpolation is used to find the first and second derivatives in IDL.

The fitted function followed closely the vertical profile of a tree crown (Figure 6) and its graph has a maximum in the neighborhood of the tree top, where the first derivative equals 0 and the second derivative is negative. Points of inflection occur

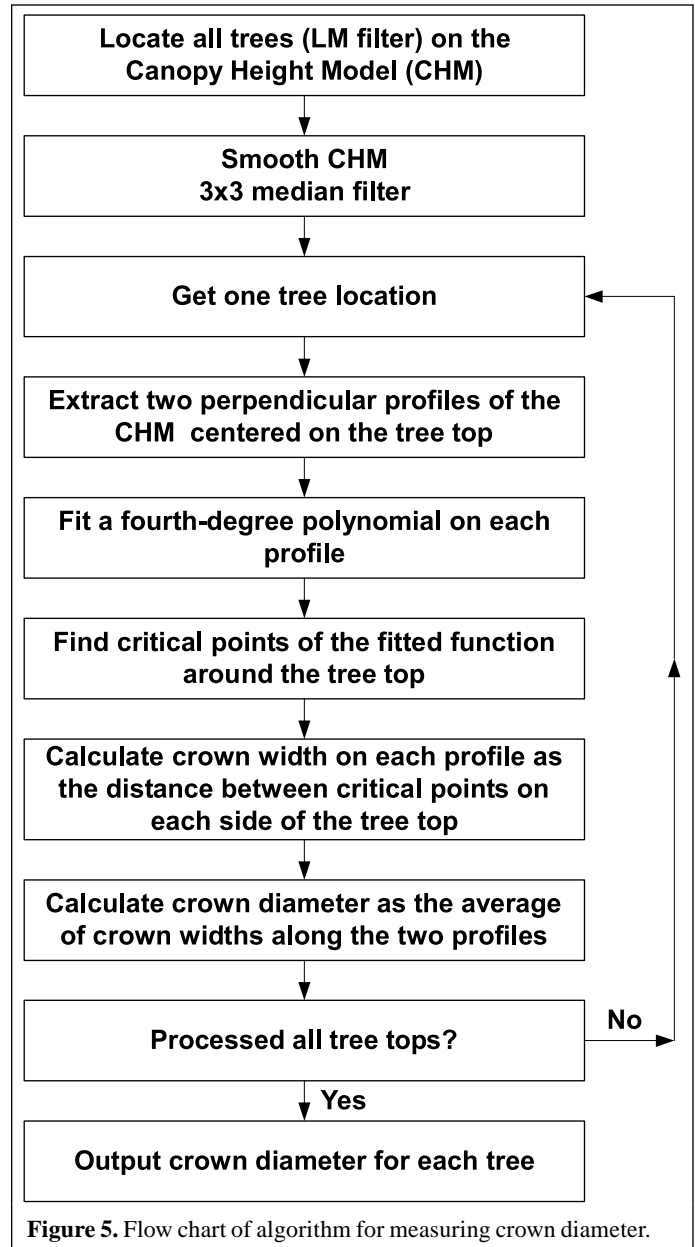


Figure 5. Flow chart of algorithm for measuring crown diameter.

on the edges of a crown profile. When these conditions were met, i.e., the fitted function indicated a tree crown profile, the distance between critical points was used to calculate the crown diameter. The final value for a crown diameter was computed as the average of the crown diameters measured on the two perpendicular directions or profiles. Owing to the complexity of the CHM, sometimes the first and second derivatives cannot provide real solutions and crown diameter cannot be measured. For 4.49% of the trees identified on the three-dimensional lidar CHM in an area with both deciduous and pine trees, the crown diameter could not be measured. As expected, in an area covered only by large deciduous trees with a complex spatial interaction between neighboring crowns, the algorithm could not calculate the crown diameter for 8.78% of the tree tops identified by the LM filter. Trees that did not have a lidar measurement for crown diameter were ignored when

computing average crown diameter per plot. This method seems appropriate to measure crown diameter for dominant and codominant trees that have individualized crowns on the CHM surface. This algorithm measures non-overlapping crown diameters, while the field measurements considers crowns to their full extent, therefore measuring overlapping crown diameters.

Regression analysis

Linear regression models were used to develop equations relating lidar-derived parameters, such as tree height, stand density, and crown width, with field inventory data of crown width for each of the FIA subplots. Subplots were pooled together in two categories, deciduous trees and pines. Stepwise multiple regression models, each with a 0.15 significance level, were developed separately for each of the two forest type

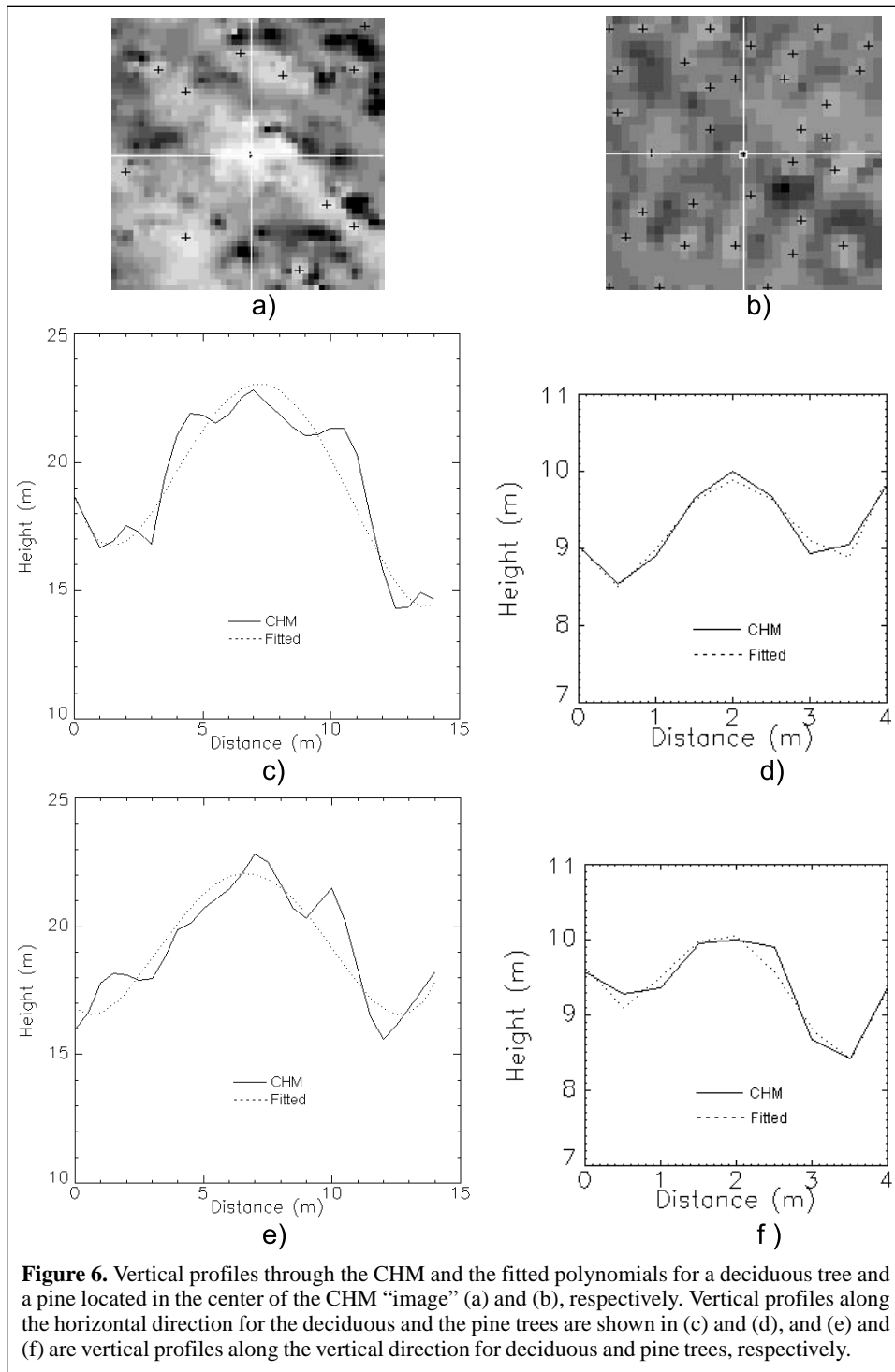


Figure 6. Vertical profiles through the CHM and the fitted polynomials for a deciduous tree and a pine located in the center of the CHM “image” (a) and (b), respectively. Vertical profiles along the horizontal direction for the deciduous and the pine trees are shown in (c) and (d), and (e) and (f) are vertical profiles along the vertical direction for deciduous and pine trees, respectively.

categories. The independent variables (**Table 4**) were the lidar measurements for each subplot, including the number of trees, average height, minimum and maximum height, average crown diameter, minimum and maximum crown diameter, and the standard deviations of height and crown diameter. The measures of height and crown diameter variability, i.e., standard deviations for height and crown diameter, were included among the independent variables as they account for the complex stand conditions within the study area. A large variance for height and crown diameter might indicate an all-aged canopy structure and it connotes larger crown diameters for the dominant and codominant trees and higher values for volume and biomass. Regression analysis was also performed with and without the independent variables related to crown diameter when investigating the effect of lidar-derived crown diameter on estimating forest volume and biomass.

The study of Popescu et al. (2002) confirmed that lidar is better suited to measure trees in the upper layer of the canopy, mainly the dominant and codominant trees. Therefore, the field-measured dependent variables for height, crown diameter, dbh, and number of trees were separated into two categories, based on the dbh: (1) all trees inventoried on the ground with measurements for crown diameter (includes trees with a dbh larger than 12.7 cm (5.0 in)), and (2) dominant and codominant trees (trees with dbh larger than the quadratic mean diameter).

The presence of multicollinearity effects was investigated using eigenvalues and eigenvectors of the correlation matrices. Multicollinearity can be measured in terms of the ratio of the largest to the smallest eigenvalue (Equation (1)), which is called the condition number of the correlation matrix (Myers, 1990). A condition number that exceeds 1000 raises concerns for multicollinearity effects. The condition number (ϕ) was calculated with the formula below:

$$\phi = \frac{\lambda_{\max}}{\lambda_{\min}} \quad (1)$$

where λ_{\max} and λ_{\min} are respectively the largest and the smallest eigenvalues.

Table 4. Regression variables.

Independent variables (lidar measured)	Predicted variables (field measured)
Tree height	
Avg. height/subplot	
Min. height	
Max. height	
SD of individual tree heights	Crown diameter (avg./subplot)
Crown diameter	
Avg. crown diameter/subplot	Volume
Min. crown diameter	Biomass
Max. crown diameter	
SD of individual tree crown diameters	
No. of trees	

Since the ground-truth data were split into pine and deciduous plots, it was not practical to split it again for validation purposes. Therefore, the PRESS (prediction sum of squares) statistic was used as a form of cross-validation, very much in the spirit of data splitting (Myers, 1990). The PRESS statistic is defined as

$$\text{PRESS} = \sum_{i=1}^n (e_{i,-i})^2 \quad (2)$$

where $e_{i,-i}$, $i = 1, \dots, n$, are prediction errors or PRESS residuals.

To calculate the PRESS statistic, one observation, in this case one subplot ground value, is set aside from the sample, and the remaining observations are used to estimate the coefficients for a particular candidate model. The observation previously set aside is then replaced and another observation withheld with coefficients estimated again. Each observation is therefore removed one at a time and the model is fitted n times, n being the number of observations in the dataset. The observation set aside is predicted each time, resulting in n prediction errors or PRESS residuals ($e_{i,-i}$, $i = 1, \dots, n$). These residuals are true prediction errors, since one observation is not simultaneously used for fit and model assessment. The PRESS statistic was calculated for the models obtained for each of the four filtering methods. In addition, the range of PRESS residuals, their mean, and standard deviation are reported for each model. For the choice of the best model, one might favor the model with the smallest PRESS.

Results and discussion

Crown diameter and tree locating method

As expected, the regression analysis indicated that the average crown diameter is less accurately estimated than the average height. Typically, crown diameter is not measured in forest inventories, but it is needed to calculate certain competition measures (Avery and Burkhart, 1994; Biging and Dobbertin, 1995) and to determine canopy cover. When needed, it is usually subsampled and estimated from other tree measurements. The study of Gill et al. (2000) developed models of tree crown radius for several conifer species of California and obtained R^2 values in the range of 0.2691 to 0.6077 and RMSE values from 0.6081 to 1.48 m. The variable with the best prediction for their models was dbh.

The regression analysis for the current study showed that results are similar for both pines and deciduous trees, with R^2 values of 0.62–0.63 for the dominant trees and a standard error of estimate of 1.36–1.41 m (**Table 5**). For pines, data fusion improved the R^2 value by 8% to 10%, while for deciduous trees the boost was more significant, from 6% to 24%. The algorithm that gave the best results for pines was the square LM filter with data fusion, while the circular LM filter with data fusion gave the best results for deciduous trees. **Figure 7** shows scatterplots of predicted vs. observed and lidar vs. field crown diameter for

Table 5. Regression results where the dependent variable is the average crown diameter (m) per subplot.

Trees	Method ^a	Significant independent variables ^b	Standard error of estimate	R ²	Model ^c
Pines					
Dominants	SQ	H_{\max}, CD_{\max}	1.49	0.5573	$1.73117 + 0.34275H_{\max} - 0.64997CD_{\max}$
	SQF	H_{\max}, CD_{\max}	1.36	0.6317	$2.53820 + 0.38918H_{\max} - 0.99219CD_{\max}$
	CW	$H_{\max}, CD_{\text{std}}$	1.46	0.5767	$0.43083 + 0.16732H_{\max} + 1.26712CD_{\text{std}}$
	CWF	H_{\max}, CD_{\max}	1.47	0.5687	$-0.51619 + 0.13903H_{\max} + 0.53766CD_{\max}$
All (FIA standard)	SQ	H_{\max}, CD_{\max}	1.29	0.5095	$2.07945 + 0.27392H_{\max} - 0.53800CD_{\max}$
	SQF	H_{\max}, CD_{\max}	1.16	0.6057	$2.85880 + 0.32246H_{\max} - 0.88105CD_{\max}$
	CW	H_{\max}, CD_{\max}	1.32	0.4903	$0.41416 + 0.11895H_{\max} + 0.35748CD_{\max}$
	CWF	H_{\max}, CD_{\max}	1.30	0.5041	$0.33285 + 0.11296H_{\max} + 0.39461CD_{\max}$
Deciduous					
Dominants	SQ	H_{ave}	1.80	0.3337	$2.04905 + 0.22828H_{\text{ave}}$
	SQF	H_{\max}	1.75	0.3513	$1.20716 + 0.25101H_{\max}$
	CW	H_{ave}	1.71	0.3833	$1.93286 + 0.24868H_{\text{ave}}$
	CWF	$H_{\text{ave}}, CD_{\text{ave}}, CD_{\text{min}}, CD_{\text{std}}$	1.41	0.6236	$0.82883 + 0.42087H_{\text{ave}} + 1.45125CD_{\text{ave}} - 1.93922CD_{\text{min}} - 1.53391CD_{\text{std}}$
All (FIA standard)	SQ	$H_{\text{ave}}, CD_{\text{ave}}$	0.99	0.4652	$2.59964 + 0.25530H_{\text{ave}} - 0.35977CD_{\text{ave}}$
	SQF	$H_{\text{ave}}, CD_{\text{ave}}$	0.98	0.4663	$2.82134 + 0.22236H_{\text{ave}} - 0.26108CD_{\text{ave}}$
	CW	H_{ave}	0.96	0.4360	$2.72765 + 0.15628H_{\text{ave}}$
	CWF	$H_{\text{ave}}, CD_{\text{min}}$	0.93	0.4930	$2.29544 + 0.21825H_{\text{ave}} - 0.19038CD_{\text{min}}$

^aMethod refers to LM filtering technique. SQ, square window; SQF, square window with data fusion; CW, circular window; CWF, circular window with data fusion.

^b H_{ave} , average height of all lidar identified trees per plot; H_{min} , minimum height; H_{max} , maximum height; H_{std} , height standard deviation; CD_{ave} , average crown diameter; CD_{min} , minimum crown diameter; CD_{max} , maximum crown diameter; CD_{std} , crown diameter standard deviation; N, number of trees.

^cAll units in meters.

the regression models that gave the best results as mentioned above.

For the pine plots, the cross-validation (**Table 6**) also showed that using the optical data improved the prediction of crown diameter, revealing overall smaller PRESS statistics and standard deviations of PRESS residuals. With square-window filtering for pines, optical data made a considerable difference in improving the estimation of crown diameter, as shown by both regression results and cross-validation. Though R^2 values were slightly better when filtering with square windows than with circular windows, prediction accuracy seems better for the latter.

For the deciduous plots, using the optical data consistently gave better results with both shapes of the filtering windows, as indicated by R^2 values and PRESS statistics. Despite the fact that for both pine and deciduous plots the R^2 values were higher when regressing the crown diameter of dominant trees, prediction accuracy was slightly better for the crown diameter of all trees measured by FIA standards. The smallest overall PRESS statistics and sub-meter standard deviation of PRESS residuals were obtained for the average crown diameter of all FIA measured trees on the deciduous plots. **Figures 7a** and **7b** show scatterplots of lidar-measured vs. field-measured crown diameter and observed vs. predicted values for crown diameter for the pine and deciduous models with the best fit and prediction.

The lidar-measured variables that proved significant for predicting crown diameter for the pine plots were maximum

height and maximum crown diameter. For the deciduous plots, most frequently average height and average crown diameter appeared as significant variables.

Part of the unexplained variance associated with crown diameter can be attributed to the fact that the algorithm for calculating crown diameter on the lidar CHM aimed at measuring the non-overlapping crown diameter, while the field measurements considered crowns to their full extent and therefore measured overlapping crown diameters. This also explains the three outliers in **Figure 7c**. All three outliers were registered on subplots with mature pine trees, with average subplot heights of 19.3, 27.4, and 30.2 m and average field-measured crown diameter of 8.79, 9.16, and 10.89 m, respectively. The number of dominant trees on these subplots was between two and four. Given a subplot radius of 7.32 m, it is evident that the crowns of these large pines overlap, while lidar only measured non-overlapping crowns. The difference between overlapping and non-overlapping crown diameters also explains the increased variance associated with the average crown diameter of deciduous plots in **Figure 7d** for larger crown diameters. A portion of the unexplained variance for crown diameter can also be attributed to errors of co-registration between lidar and ground plots, influenced by both lidar positioning accuracy and GPS errors for locating ground plots. However, with an increased sampling intensity of lidar, the CHM should better portray the three-dimensional model of the tree crown and as a consequence, predicting crown diameter should become more accurate.

Table 6. PRESS statistics for predicting average crown diameter (m) per subplot.

Trees	Method ^a	PRESS	Range of PRESS residuals		Mean of PRESS residuals	SD of PRESS residuals
			Min.	Max.		
Pines						
Dominants	SQ	88.56	-3.69	5.31	0.14	1.84
	SQF	59.39	-3.49	4.25	0.08	1.51
	CW	53.09	-2.71	3.13	0.02	1.43
	CWF	50.21	-2.73	3.01	0.04	1.39
All (FIA Standard)	SQ	67.37	-2.43	5.42	0.12	1.60
	SQF	45.72	-2.09	4.52	0.10	1.32
	CW	43.38	-2.31	3.78	0.05	1.29
	CWF	43.34	-2.24	3.64	0.08	1.29
Deciduous						
Dominants	SQ	91.32	-2.49	5.50	0.00	1.91
	SQF	91.08	-4.00	4.95	0.00	1.87
	CW	93.72	-2.79	5.26	0.00	1.80
	CWF	88.06	-2.55	3.86	0.10	1.74
All (FIA Standard)	SQ	27.64	-1.78	2.13	0.02	1.05
	SQF	27.80	-2.03	2.05	0.02	1.03
	CW	29.40	-1.58	2.06	-0.01	1.01
	CWF	28.15	-1.96	2.26	-0.01	0.98

^aMethod refers to LM filtering technique. SQ, square window; SQF, square window with data fusion; CW, circular window; CWF, circular window with data fusion.

Influence of lidar-derived crown diameter on volume and biomass

The volume of trees in a forest is one of the most important statistics in forest management. The individual tree volume is usually considered to be a function of tree dbh, tree height, and an expression of tree form (Clutter et al., 1983), but most practitioners prefer to use volume equations that involve only dbh and height.

Total tree volume was calculated from the ground measurements for each inventoried tree. Subplot volume was derived as the sum of individual trees within the plot. For all tree species, volume equations used to calculate total outside bark tree volume were of the form (Schumacher and Hall, 1933)

$$V_t = \beta D^\gamma H^\delta \quad (3)$$

where V_t is the total outside bark volume, D is the diameter at breast height (dbh), H is the total tree height, and β , γ , δ are the parameters usually estimated from the data.

Parameter values for the tree species inventoried on the ground were found for loblolly pines in Sharma and Oderwald (2001), for southern pines in Saucier and Clark (1985), and for hardwoods species in Clark et al. (1986).

A more detailed discussion of estimating forest volume and biomass with lidar will be provided by the authors in a future publication. However, all regression models for estimating volume, with one exception for pines (when filtering with square windows) and one for hardwoods (when filtering with

square windows and data fusion), included lidar estimates of the average crown diameter. For the pine plots, crown diameter alone was able to explain up to almost 83% of the variance associated with total volume. For the deciduous plots, maximum height and average crown diameter provided the best fit ($R^2 = 0.3884$). The decrease in R^2 values when estimating volume without using lidar-measured crown diameter variables was on average 0.09, with a maximum of 0.25 for regressing volume for deciduous plots (RMSE decreased by up to 8 m³/ha).

Biomass estimated from ground measurements was obtained using dbh only, since previous studies (Crow, 1971; Schroeder et al., 1997) proved that dbh is the most reliable variable for biomass estimation. For the deciduous and coniferous species found in the Appomattox–Buckingham State Forest, biomass was calculated by using the models provided by Schroeder et al. (1997).

When estimating biomass for pines, the differences between the four processing methods were small; all models explained more than 78% of the variance. For deciduous plots, the explanatory power of the lidar-derived metrics for predicting biomass is lower than it is for pines, with the highest R^2 of 0.3276 (RMSE of 44.41 Mg/ha) obtained with the model for the circular LM filter.

All the regression models for pines and the model with the highest R^2 value for deciduous plots included lidar estimates of the average crown diameter. For the pine plots, the average lidar-derived crown diameter (circular windows filter) alone explained 78% of the variance associated with biomass. The decrease in R^2 values when predicting biomass without using

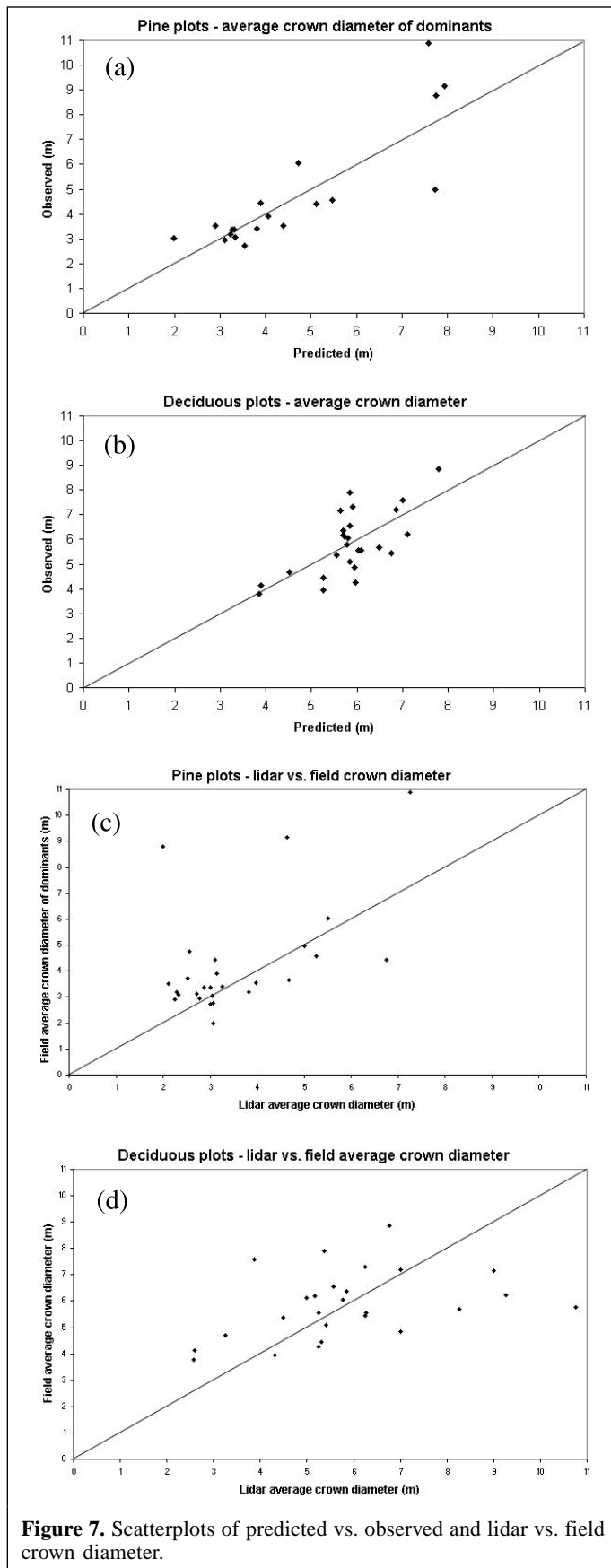


Figure 7. Scatterplots of predicted vs. observed and lidar vs. field crown diameter.

lidar-measured crown diameter variables was on average 0.11, with a maximum of 0.24 for regressing biomass for deciduous plots (RMSE decreased by up to 7 Mg/ha).

The significant impact of crown diameter in explaining the variation noted in ground-measured tree volume and biomass is of high interest for practical volume estimation using remote sensing techniques with optical and lidar data. Perfecting algorithms for measuring crown diameter on remote sensing images and increasing the lidar sampling density could significantly improve volume estimates in operational forest inventories.

Conclusions

The results of the current study show that lidar data could be used to estimate the average crown diameter and to improve estimates of other forest biophysical parameters of interest by focusing at the individual tree level. The generation of individual tree crown forest inventories from high spectral and spatial resolution imagery, although still a research subject, is coming of age (Gougeon et al., 2001). In this context, lidar is a technology well-suited to derive accurate models of the terrain elevation and measure the height of the dominant and codominant trees in the forest canopy.

Overall, this research proved that small-footprint airborne lidar data in conjunction with spatially coincident optical data are able to predict crown diameter for forest inventory and assessment. Furthermore, plot level crown diameters calculated from individual tree lidar measurements were particularly important in contributing to model fit and prediction for volume and biomass. From an historical perspective it has been argued that crown diameter is more accurately measured on large-scale photographs than on the ground (Wynne, 2003). Deriving visible crown diameter with photogrammetric techniques has some limitations due to observing only the dominant overstory trees and the shadowing effects they cast on other smaller crowns. However, photo-derived crown diameter better correlates with actual tree and stand volume than field-based measured crown diameter because it is a measure of the tree's "functional growing space" (Spurr, 1960). As opposed to photo-derived measurements, lidar offers the possibility to automatically derive biophysical parameters on large areas. Therefore, seeing the trees in the forest and more importantly measuring them with lidar brings an important contribution to concepts such as precision forest inventory and automated data processing for forestry applications.

The integration with coregistered multi- and hyper-spectral digital imagery makes lidar a realistic alternative to traditional measurements in forest inventory. Newer lidar systems have pulse rates exceeding 50 kHz plus the capacity to record both the time and intensity of multiple returns or even the full waveform. Given these developments, it is likely that data acquired from the next generation of lidar sensors will prove even more accurate for estimating forest biophysical parameters of interest. It is therefore expected that the transition from research to practical applications and

operational use of lidar in forestry will accelerate. The focus of this research on the individual tree level demonstrates that airborne laser provides the tool to reliably measure not only tree height but also crown dimensions, thus improving estimates of forest volume and biomass.

References

- Avery, T.E., and Burkhart, H.E. 1994. *Forest Measurements*. 4th ed. McGraw-Hill, Inc., New York.
- Barbezat, V., and Jacot, J. 1999. The CLAPA project: automated classification of forest with aerial photographs. In *Proceedings of the International Forum on Automated Interpretation of High Spatial Resolution Digital Imagery for Forestry*, 10–12 February 1998, Victoria, B.C. Pacific Forestry Center, Canadian Forest Service, Natural Resources Canada. pp. 345–356.
- Biging, G.S., and Dobbertin, M. 1995. Evaluation of competition indices in individual tree growth models. *Forest Science*, Vol. 41, No. 2, pp. 360–377.
- Blair, B.J., Rabine, D.L., and Hofton, M.A. 1999. The laser vegetation imaging sensor: a medium-altitude, digitisation-only, airborne laser altimeter for mapping vegetation and topography. *ISPRS Journal of Photogrammetry and Remote Sensing*, Vol. 54, No. 2–3, pp. 115–122.
- Clark, A., III, Phillips, D.R., and Frederick, D.J. 1986. *Weight, volume, and physical properties of major hardwood species in the Piedmont*. Southeastern Forest Experiment Station Research, USDA Forest Service. Technical paper SE-255.
- Clutter, J.L., Fortson, J.C., Pienaar, L.V., Brister, G.H., and Bailey, R.L. 1983. *Timber management: a quantitative approach*. John Wiley & Sons Inc., New York.
- Corvallis Microtechnology, Inc. 2001. *CMT Products – HP-GPS-L4*. Available from <<http://www.cmtinc.com/nav/frprod.html>> [accessed 30 October 2001].
- Crow, T.R. 1971. Estimation of biomass in an even-aged stand — Regression and “mean tree” techniques. In *Proceedings of the 15th IUFRO Congress, Section 25, Forest Biomass Studies*, 15–20 March 1971, Gainesville, Fla. University of Maine, Orono, Maine. pp. 35–48.
- Daley, N.M.A., Burnett, C.N., Wulder, M., Niemann, L.O., and Goodenough, D.G. 1998. Comparison of fixed-size and variable-sized windows for the estimation of tree crown position. In *Proceedings of IGARSS '98*, 6–10 July 1998, Seattle, Wash. Geoscience and Remote Sensing Society, IEEE, New York. pp. 1323–1325.
- EarthData, Inc. 2003. *Shedding new light on the Earth's terrain: Lidar*. Available from <<http://www.earthdata.com/index2.htm>> [accessed 17 February 2003].
- Erdas, Inc. 1997. *Erdas Imagine – Erdas Field Guide*. 4th ed. [computer program]. Erdas, Inc., Atlanta, Ga. p. 192.
- Eyre, F.H. 1980. *Forest cover types of the United States and Canada*. Society of American Foresters, Bethesda, Md.
- Gill, S.J., Biging, G.S., and Murphy, E.C. 2000. Modeling conifer tree crown radius and estimating canopy cover. *Forest Ecology and Management*, Vol. 126, pp. 405–416.
- Gillett, P. 1984. *Calculus and analytic geometry*. 2nd ed. D.C. Heath and Company, Boston. p. 188.
- Gougeon, F. 1999. Automatic individual tree crown delineation using a valley-following algorithm and a rule-based system. In *Proceedings of the International Forum on Automated Interpretation of High Spatial Resolution Digital Imagery for Forestry*, 10–12 February 1998, Victoria, B.C. Pacific Forestry Center, Canadian Forest Service, Natural Resources Canada. pp. 11–23.
- Gougeon, F.A., St-Onge, B.A., Wulder, M., and Leckie, D.G. 2001. Synergy of airborne laser altimetry and digital videography for individual tree crown delineation. In *Proceedings of the 23rd Canadian Symposium on Remote Sensing – 10^e Congrès de l'Association québécoise de télédétection*, 21–24 August 2001, Québec, Que. CASI, Ottawa, Ont.
- Harding, D.J., Blair, J.B., Garvin, J.B., and Laurence, W.T. 1994. Laser altimetry waveform measurement of vegetation canopy structure. In *Proceedings of the International Geoscience and Remote Sensing Symposium – IGARSS '94*. ESA Scientific & Technical Publication, Noordwijk, Netherlands. pp. 1251–1253.
- Holmgren, J., Nilsson, M., and Olsson, H. 2003. Estimation of tree height and stem volume on plots using airborne laser scanning. *Forest Science*, Vol. 49, No. 3, pp. 409–418.
- Lefsky, M.A., Cohen, W.B., Acker, S.A., Spies, T.A., Parker, G.G., and Harding, D. 1997. Lidar remote sensing of forest canopy structure and related biophysical parameters at the H.J. Andrews experimental forest, Oregon, U.S.A. In *Natural resources management using remote sensing and GIS*. Edited by J.D. Greer. ASPRS, Washington, D.C. pp. 79–91.
- Lefsky, M.A., Harding, D., Cohen, W.B., Parker, G., and Shugart, H.H. 1999. Surface lidar remote sensing of basal area biomass in deciduous forests of eastern Maryland, U.S.A. *Remote Sensing of Environment*, Vol. 67, pp. 83–98.
- Maclean, G.A., and Krabill, W.B. 1986. Gross-merchantable timber volume estimation using an airborne LIDAR system. *Canadian Journal of Remote Sensing*, Vol. 12, No. 1, pp. 7–18.
- Magnussen, S., and Boudewyn, P. 1998. Derivations of stand heights from airborne laser scanner data with canopy-based quantile estimators. *Canadian Journal of Forest Research*, Vol. 28, pp. 1016–1031.
- Magnussen, S., Eggermont, P., and LaRiccica, V.N. 1999. Recovering tree heights from airborne laser scanner data. *Forest Science*, Vol. 45, No. 3, pp. 407–422.
- McCombs, J.W., Roberts, S.D., and Evans, D.L. 2003. Influence of fusing lidar and multispectral imagery on remotely sensed estimates of stand density and mean tree height in a managed loblolly pine plantation. *Forest Science*, Vol. 49, No. 3, pp. 457–466.
- Means, J.E., Acker, S.A., Harding, D.J., Blair, J.B., Lefsky, M.A., Cohen, W.B., Harmon, M.E., and McKee, W.A. 1999. Use of large-footprint scanning airborne lidar to estimate forest stand characteristics in the Western Cascades of Oregon. *Remote Sensing of Environment*, Vol. 67, pp. 298–308.
- Myers, R.H. 1990. *Classical and modern regression with applications. The Duxbury advanced series in statistics and decision sciences*. PWS-Kent, Boston. pp. 171–178, 370.
- Næsset, E. 1997a. Determination of mean tree height of forest stands using airborne laser scanner data. *ISPRS Journal of Photogrammetry and Remote Sensing*, Vol. 52, pp. 49–56.
- Næsset, E. 1997b. Estimating timber volume of forest stands using airborne laser scanner data. *Remote Sensing of Environment*, Vol. 61, No. 2, pp. 246–253.
- Næsset, E., and Bjercknes, K.-O. 2001. Estimating tree heights and number of stems in young forest stands using airborne laser scanner data. *Remote Sensing of Environment*, Vol. 78, pp. 328–340.

- Næsset, E., and Økland, T. 2002. Estimating tree height and tree crown properties using airborne scanning laser in a boreal nature reserve. *Remote Sensing of Environment*, Vol. 79, pp. 105–115.
- Nelson, R.F. 1997. Modeling forest canopy heights: the effects of canopy shape. *Remote Sensing of Environment*, Vol. 60, pp. 327–334.
- Nelson, R.F., Krabill, W.B., and Maclean, G.A. 1984. Determining forest canopy characteristics using airborne laser data. *Remote Sensing of Environment*, Vol. 15, pp. 201–212.
- Nelson, R.F., Swift, R., and Krabill, W. 1988a. Using airborne lasers to estimate forest canopy and stand characteristics. *Journal of Forestry*, Vol. 86, pp. 31–38.
- Nelson, R.F., Krabill, W., and Tonelli, J. 1988b. Estimating forest biomass and volume using airborne laser data. *Remote Sensing of Environment*, Vol. 24, pp. 247–267.
- Pinz, A. 1999. Tree isolation and species classification. In *Proceedings of the International Forum on Automated Interpretation of High Spatial Resolution Digital Imagery for Forestry*, 10–12 February 1998, Victoria, B.C. Pacific Forestry Center, Canadian Forest Service, Natural Resources Canada. pp. 127–139.
- Popescu, S.C. 2002. *Estimating plot-level forest biophysical parameters using small-footprint airborne lidar measurements*. Ph.D. dissertation, Virginia Polytechnic Institute and State University, Blacksburg, Va.
- Popescu, S.C., and Wynne, R.H. 2001. Estimating tree heights and stand density with high performance lidar: Initial results from a case study in the Virginia Piedmont. In *Proceedings of the American Society for Photogrammetry and Remote Sensing 2001 Annual Conference*, 23–27 April 2001, St. Louis, Mo.
- Popescu, S.C., and Wynne, R.H. 2003. Seeing the trees in the forest: using lidar and multispectral data fusion with local filtering and variable window size for estimating tree height. *Photogrammetric Engineering & Remote Sensing*. In press.
- Popescu, S.C., Wynne, R.H., and Nelson, R.H. 2000. Estimating forest vegetation biomass using airborne lidar measurements. In *Proceedings of the Second International Conference on Geospatial Information in Agriculture and Forestry*, 10–12 January 2000, Lake Buena Vista, Fla. ERIM International, Inc., Ann Arbor, Mich. pp. 346–353.
- Popescu, S.C., Wynne, R.H., and Nelson, R.H. 2002. Estimating plot-level tree heights with lidar: local filtering with a canopy-height based variable window size. *Computers and Electronics in Agriculture*, Vol. 37, No. 1–3, pp. 71–95.
- Powell, D.S., Faulkner, J.L., Darr, D.R., Zhou, Z., and MacCleerry, D.W. 1993. *The forest resources in the United States, 1992*. USDA Forest Service General Technical Report RM-234. 132 pp.
- Press, W.H., Teukolsky, S.A., Vetterling, W.T., and Flannery, B.P. 1992. *Numerical recipes in C: the art of scientific computing*. 2nd ed. Cambridge University Press, New York. p. 676.
- St-Onge, B.A., and Cavayas, F. 1995. Estimating forest stand structure from high resolution imagery using the directional variogram. *International Journal of Remote Sensing*, Vol. 16, No. 11, pp. 1999–2021.
- Saucier, R.J., and Clark, A., III. 1985. *Tables for estimating total tree and product weight and volume of major southern tree species and species groups*. Southwide Energy Committee, American Pulpwood Association, Inc., Rockville, Md.
- Schroeder, P., Brown, S., Mo, J., Birdsey, R., and Cieszewski, C. 1997. Biomass estimation for temperate broadleaf forests of the United States using inventory data. *Forest Science*, Vol. 43, pp. 424–434.
- Schumacher, F.X., and Hall, F.D.S. 1933. Logarithmic expression of timber-tree volume. *Journal of Agriculture Research*, Vol. 47, pp. 719–734.
- Sharma, M., and Oderwald, R.G. 2001. Dimensionally compatible volume and taper equations. *Canadian Journal of Forest Research*, Vol. 31, No. 5, pp. 797–803.
- Spurr, S.H. 1960. *Photogrammetry and Photo-Interpretation with a Section on Applications to Forestry*. Ronald Press, New York. p. 366.
- U.S. Department of Agriculture – Forest Service. 2001. *Forest inventory and analysis national core field guide, Volume 1: Field data collection procedures for phase 2 plots, Version 1.5*. U.S. Department of Agriculture, Forest Service, Forest Inventory and Analysis, Washington Office. Internal report.
- Weishampel, J.F., Harding, D.J., Boutet, J.C. Jr., and Drake, J.B. 1997. Analysis of laser altimeter waveforms for forested ecosystems of central Florida. In *Proceedings of the SPIE Conference on Advances in Laser Remote Sensing for Terrestrial and Oceanographic Applications*, 21–25 April, Orlando, Fla. SPIE, Bellingham, Wash. Vol. 3059, pp. 184–189.
- Wulder, M., Niemann, K.O., and Goodenough, D.G. 2000. Local maximum filtering for the extraction of tree locations and basal area from high spatial resolution imagery. *Remote Sensing of Environment*, Vol. 73, pp. 103–114.
- Wynne, R.H. 2003. Forest mensuration with remote sensing: A retrospective with a vision for the future. *Southern Forest Science: Past, Present, Future*. U.S. Government Printing Office, Washington, D.C. In press.